Mon. Not. R. Astron. Soc. **399,** L39–L43 (2009) doi:10.1111/j.1745-3933.2009.00720.x

Cosmological and astrophysical constraints from the Lyman α forest flux probability distribution function

Matteo Viel,[1,2]★ James S. Bolton[3] and Martin G. Haehnelt[4,5]

[1]*INAF – Osservatorio Astronomico di Trieste, Via G.B. Tiepolo 11, I-34131 Trieste, Italy*
[2]*INFN/National Institute for Nuclear Physics, Via Valerio 2, I-34127 Trieste, Italy*
[3]*Max-Planck-Institut für Astrophysik, Karl-Schwarzschild Str. 1, 85748 Garching, Germany*
[4]*Institute of Astronomy, Madingley Road, Cambridge CB3 0HA*
[5]*KICC – Kavli Institute of Cosmology, Madingley Road, Cambridge CB3 0HA*

Accepted 2009 July 14. Received 2009 July 14; in original form 2009 June 19

ABSTRACT

We use the probability distribution function (PDF) of the Lyman α forest flux at $z = 2$–3, measured from high-resolution UVES/VLT data, and hydrodynamical simulations to obtain constraints on cosmological parameters and the thermal state of the intergalactic medium (IGM) at $z \sim 2$–3. The observed flux PDF at $z = 3$ alone results in constraints on cosmological parameters in good agreement with those obtained from the *Wilkinson Microwave Anisotropy Probe* (*WMAP*) data, albeit with about a factor of 2 larger errors. The observed flux PDF is best fit with simulations with a matter fluctuation amplitude of $\sigma_8 = 0.8$–0.85 ± 0.07 and an inverted IGM temperature–density relation ($\gamma \sim 0.5$–0.75), consistent with our previous results obtained using a simpler analysis. These results appear to be robust to uncertainties in the quasar (quasi-stellar object) continuum placement. We further discuss constraints obtained by a combined analysis of the high-resolution flux PDF and the power spectrum measured from the Sloan Digital Sky Survey (SDSS) Lyman α forest data. The joint analysis confirms the suggestion of an inverted temperature–density relation, but prefers somewhat higher values ($\sigma_8 \sim 0.9$) of the matter fluctuation amplitude than the *WMAP* data and the best fit to the flux PDF alone. The joint analysis of the flux PDF and power spectrum (as well as an analysis of the power spectrum data alone) prefers rather large values for the temperature of the IGM, perhaps suggesting that we have identified a not yet accounted for systematic error in the SDSS flux power spectrum data or that the standard model describing the thermal state of the IGM at $z \sim 2$–3 is incomplete.

Key words: methods: numerical – intergalactic medium – cosmology: theory.

1 INTRODUCTION

The Lyman α forest is an important cosmological observable that probes matter density fluctuations in the intergalactic medium (IGM) over a unique range of redshifts, scales and environments. Many attempts have been made to measure physical properties of the IGM using Lyman α forest data. The two most common approaches are either based on decomposing the information encoded in the transmitted flux via Voigt profile fitting or treating the flux as a continuous field with directly measurable statistical properties (e.g. Rauch et al. 1997; Rauch 1998; Theuns et al. 1998; Croft et al. 2002; Meiksin 2007). In the second approach, measurement of the zero, one, two- or three-point probability distribution functions (PDFs; i.e. the mean flux level, the flux PDF, the flux power and bispectrum) enable a variety of physical properties to be explored. The mean flux level, for example, is sensitive to the amplitude of the metagalactic ultraviolet background (Tytler et al. 2004; Bolton et al. 2005) while the flux PDF is sensitive to the thermal evolution of the IGM (Bolton, Oh & Furlanetto 2009b; McQuinn et al. 2009). The flux power spectrum (PS) has been used to constrain cosmological parameters and the behaviour of dark matter at small scales (Viel, Haehnelt & Springel 2004; Seljak, Slosar & McDonald 2006; Viel et al. 2008) and the flux bispectrum can be used to search for signatures of non-Gaussianities in the matter distribution (Viel et al. 2009). Ideally, a given IGM model described by a set of cosmological and astrophysical parameters should agree with all these statistics including the results from Voigt profile decomposition at the same time. In practice, the interpretation of the data is complex and is heavily dependent on numerical simulations that incorporate the relevant physical ingredients, but have a limited dynamic range.

★E-mail: viel@oats.inaf.it

The data used for these investigations consist mainly of two kinds of sets of quasi-stellar object (QSO) spectra: the Sloan Digital Sky Survey (SDSS) low-resolution, low signal-to-noise ratio (S/N) sample and UVES/Very Large Telescope (VLT) or HIRES/KECK samples of high-resolution spectra. The characteristics of the low- and high-resolution data sets are very different (the number of SDSS spectra is about a factor of ∼200 larger than that of high-resolution samples, but the latter probes smaller scales due to the higher spectral resolution). Measurements based on Lyman α forest data have reached a level of accuracy where an understanding of systematic uncertainties at the per cent level or below (the magnitude of statistical errors associated with the SDSS sample) has become important. In this Letter, we will revisit the flux PDF, which has been investigated previously by several authors either on its own (e.g. McDonald et al. 2000; Jena et al. 2005; Becker, Rauch & Sargent 2007; Lidz et al. 2006; Kim et al. 2007, hereafter K07; Bolton et al. 2008, herafter B08) or jointly with the flux PS (Meiksin, Bryan & Machacek 2001; Zaroubi et al. 2006; Desjacques, Nusser & Sheth 2007). We will focus on the flux PDF of the UVES/VLT data as recently measured by K07; the systematic and statistical errors for this sample have been addressed in detail. Recently, both B08 (from the K07 UVES/VLT data) and Becker et al. (2007) (from independent HIRES/KECK spectra) have found evidence for a density–temperature relation of the IGM which appears inverted if approximated as a power law [$\gamma < 1$ for $T = T_0(1 + \delta)^{\gamma-1}$]. Here, we will improve on the analysis performed in B08 and check its robustness by fully exploring the cosmological and astrophysical parameter space. In addition, we briefly discuss a joint analysis of the flux PDF and SDSS flux PS, and the possible implications for constraints on cosmological parameters describing the linear matter PS and the thermal history of the IGM.

2 METHOD

We use simulations performed with the parallel hydrodynamical (TREESPH) code GADGET-2 (Springel 2005) to calculate the flux statistics for models with a wide range of cosmological and astrophysical parameters by expanding around a reference model. For the reference model, we choose here the 20-256 simulation of B08. We refer the reader to this Letter for further details, including resolution and box size convergence tests (see Bolton & Becker 2009 for recent convergence tests on smoothed particle hydrodynamics simulations). We will compare these simulations to improved measurements of the PDF made by K07 in three redshift bins at $\langle z \rangle = 2.07, 2.52$ and 2.94 based on a set of 18 high resolution ($R \sim 45\,000$), high signal-to-noise ratio (S/N $\geq$ 30–50) VLT/UVES spectra. Further details regarding the observational data and its reduction, with particular emphasis on metal removal and continuum fitting errors, may be found in K07. In all instances, the mock QSO spectra have been processed to have the same instrumental properties as the observed data: i.e. the same S/N, resolution and pixel size.

We explore the following cosmological and astrophysical parameters: $\Omega_{\rm m}, n_{\rm s}, H_0, \sigma_8$ for the cosmological part and $T_0^{A,S}$ $(z = 3)$ and $\gamma^{A,S}$ $(z = 3)$ for the IGM thermal history, where A and S indicate the amplitude and slope for the temperature and γ relations normalized at $z = 3$ $\{y = A[(1 + z)/4]^S\}$. The amplitude and slope of the effective optical depth evolution, $\tau_{\rm eff} = -\langle F \rangle$, are varied assuming a power-law evolution with redshift in order to conservatively span the observed range suggested by high-resolution and low-resolution data sets. We furthermore varied the reionization redshift ($z_{\rm re} = 9$ in our reference model) but found this had no impact on the flux PDF at $z < 3$ (although the differences in 'Jeans smoothing' will be important at redshifts close to $z_{\rm re}$; e.g. Pawlik, Schaye & van Scherpenzeel 2009). For the effect on the flux power, we refer to McDonald et al. (2005) and Viel & Haehnelt (2006). We also consider the effect of a misplaced continuum level by adding an extra parameter $f_{\rm c}$ [the flux following a continuum correction is assumed to be $F\ (1 + f_{\rm c})$].

We compute derivatives of the flux statistics from the 20-256 model at second order using between two and four simulations for each cosmological and astrophysical parameter. For the thermal history, we explore a wide range of possible T_0 and γ values by extending the original grid of simulations presented in B08. The 20-256 model has $\gamma \sim 1.3$ below $z = 3$, and the temperature at mean density in the three PDF redshift bins are $T_0 = 14.8, 17.6, 20.8 \times 10^3$ K. This model was shown to be a poor fit to the K07 data in the simple analysis performed by B08. Here, we will calculate the χ^2 of our models varying *all* the parameters that affect the flux PDF and not just the effective optical depth, enabling us to expand around this model. This simple Taylor-expansion method was introduced in Viel & Haehnelt (2006) in order to explore constraints for the SDSS flux PS. It has the advantage of enabling the exploration of the parameter space close to the reference model with an accurate set of hydrodynamical simulations. However, the full parameter space cannot be probed in this way with the same high accuracy (see McDonald et al. 2005 for a different approach).

3 RESULTS FOR THE FLUX PDF

We obtain the best fit to the observed flux PDF for three flux intervals $F = [0.1–0.8]$, $[0.1–0.9]$, $[0–1]$. Different flux levels are subject to different systematic effects, such as the presence of noise and strong absorption systems at $F \sim 0$ and the effect of continuum fitting errors at $F \sim 1$ (see K07 for details). Since the PDF error bars are correlated, we expect these systematic errors to nevertheless impact on the PDF over the full flux range. The level of consistency between the fits to these three flux intervals should indicate to what extent these systematic errors may or may not affect the results.

For the flux range $F = [0.1–0.8]$, we have a total of 45 data points to fit and a set of nine free parameters that will be varied in the Markov Chain Monte Carlo routines. We use the following priors on the effective optical depth, $\tau_{\rm eff}^A = 0.36 \pm 0.11$ and $\tau_{\rm eff}^S = 3.65 \pm 0.21$, based on the observational results obtained by K07. Note, however, that the final results are affected very little by the choice of these priors; the constraints on the effective optical depth amplitude at $z = 3$ are in fact much tighter than these priors assume. The results of this analysis are summarized in Table 1 and Figs 1 and 2. We obtain a very good fit to the flux PDF for the flux range $F = [0.1–0.8]$ (reduced $\chi^2 = 0.98$, a χ^2 larger than this has 50 per cent probability). With the data points at $F < 0.1$, we obtain slightly larger values for σ_8 and T_0, but the results are in agreement at the 1σ level. Adding the flux range at $F > 0.9$ results in a poor fit unless the error bars on the last two data points are increased by a factor of 4. Note that the covariance properties of these data points are strongly influenced by the choice of the continuum level. Increasing the error bars by this factor would account for a misplacement of the continuum level by a few per cent. We also find evidence (2σ) that the data prefer a non-zero continuum offset, $f_{\rm c}$, when we add the regions at low and high transmissivity, but note that realistic errors in the assumed continuum level should depend on the flux and noise level and are expected to vary along the spectrum.

In order to further explore the sensitivity to the last two data points ($F = 0.95, 1$) in each redshift bin, we performed an additional

Table 1. Marginalized cosmological and astrophysical parameters derived from fitting the flux PDF at $z = 2.07$, 2.52, 2.94 in the flux ranges $F =$ [0.1–0.8], [0.1–0.9] and [0–1] (left-hand, middle and right-hand columns, respectively): T_0 is measured in units of 10^3 K; H_0 in km s^{-1} Mpc^{-1}.

Parameter	$(20,256)^{0.1-0.8}$	$(20,256)^{0-0.9}$	$(20,256)^{0-1}$
σ_8	0.81 ± 0.07 (0.80)	0.85 ± 0.07	0.86 ± 0.06
n_s	0.96 ± 0.03 (0.95)	0.96 ± 0.03	0.96 ± 0.03
Ω_{0m}	0.23 ± 0.07 (0.19)	0.22 ± 0.06	0.22 ± 0.06
H_0	82 ± 7 (80)	84 ± 6	85 ± 8
T_0	19 ± 6 (15)	24 ± 8	26 ± 7
T_0^{s1}	0.6 ± 1.4 (-0.6)	1.3 ± 1.2	1.5 ± 1.0
γ^A	0.75 ± 0.21 (0.72)	0.51 ± 0.13	0.51 ± 0.13
γ^{s1}	-1.0 ± 1.0 (-1.7)	-1.6 ± 0.9	-1.3 ± 1.0
$\tau_{\rm eff}^A$	0.312 ± 0.012 (0.312)	0.321 ± 0.010	0.324 ± 0.010
$\tau_{\rm eff}^{s1}$	3.17 ± 0.18 (3.20)	3.16 ± 0.13	3.25 ± 0.14
$f_c \times 100$	0 ± 1 (0)	-0.8 ± 0.4	-1 ± 0.4
χ^2/d.o.f.	35.2/36	45.6/48	64/54

Note. The probabilities of having a χ^2 larger than the obtained values are 50, 57 and 17 per cent, respectively. The values in parentheses are best-fitting values for $(20,256)^{[0.1-0.8]}$.

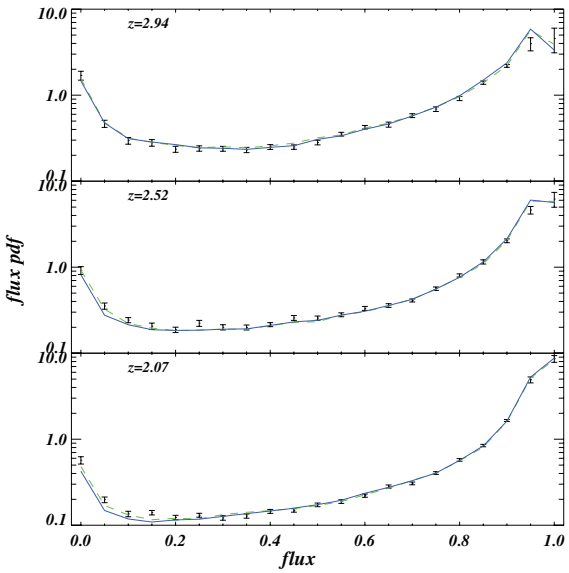

Figure 1. Best fit to the flux PDF for model $(20\text{-}256)^{0.1-0.8}$ (continuous blue) and $(20\text{-}256)^{0-1}$ (dashed green) in the three redshift bins at $\langle z \rangle =$ (2.07, 2.52, 2.94).

analysis by combining the two data points for the highest flux levels into one point at $F = 0.975$. We then recomputed the data covariance matrix and the PDF derivatives (without multiplying the covariance values of this data point by 4). In this instance, the results are consistent with those for the $F =$ [0–0.9] and [0–1] flux ranges, range to within 1σ. In this case, we obtain $\chi^2 = 60.6$ for 51 degrees of field (d.o.f.), which indicates a reasonable fit (the probability for a value larger than this is 17 per cent). We therefore conclude from the results in Table 1 that our findings are robust to continuum fitting uncertainties and that the impact of continuum uncertainties is mainly restricted to the flux range $F = 0.975$–1.025.

The effective optical depth is constrained very well by the data with a best-fitting value of $\tau_{\rm eff}(z = 3) = 0.31 \pm 0.01$, consistent with observational measurements from high-resolution spectra. The constraints on the temperature density relation at $z = 3$ are

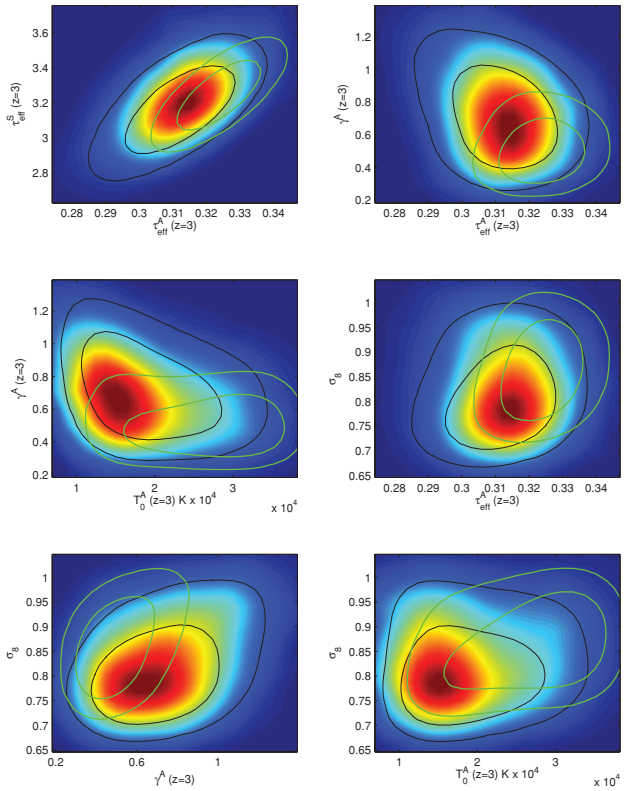

Figure 2. Two-dimensional marginalized and mean likelihood contours for cosmological and astrophysical parameters for flux PDF model $(20,256)^{0.1-0.8}$ (continuous curves and filled contours). Marginalized likelihoods for the model $(20, 256)^{0-1}$ are also shown in green.

$(T_0^A, \gamma^A) = (19 \pm 6\,, 0.75 \pm 0.21)$, in agreement with the findings of B08, and no significant evolution in the equation of state below $z < 3$ is inferred (in agreement with Schaye et al. 2000; Ricotti, Gnedin & Shull 2000). The PDF alone provides interesting constraints on cosmological parameters describing the evolution of the linear PS; σ_8 and n_s are constrained to be in the range $\sigma_8 = 0.8 - 0.85 \pm 0.07$ and $n_s = 0.96 \pm 0.03$. The derived cosmological parameters are in good agreement with the results of other large-scale structure probes such as *Wilkinson Microwave Anisotropy Probe* (*WMAP*) and weak-lensing data, albeit with about a factor of 2 larger errors than those from the *WMAP* data (e.g. Lesgourgues et al. 2007).

Our results corroborate the suggestion of an inverted temperature–density relation at $z = 3$. As for the analysis of the full flux range the statistical significance of the data favouring an inverted temperature–density relation $\gamma < 1$ is about 3σ at $z \sim 3$. At $z < 3$, the data are consistent with an isothermal ($\gamma \sim 1$) temperature–density relation The results regarding the thermal state of the IGM do not change significantly if we omit the flux range $F > 0.9$. If we discard both the flux ranges at low and high emissivity and consider only the flux range $F = [0.1-0.8]$, there is still evidence for an inverted $T - \rho$ relation, but at a reduced level of significance ($1-1.5\sigma$ confidence level). The likelihood contours in Fig. 2 indicate that a value of $\gamma \sim 1.3$ suggested recently by the He II reionization simulations of McQuinn et al. (2009) is between 2 and $3\text{–}3.5\sigma$ discrepant with the marginalized value we obtain when fitting the flux range $F = [0.1-0.8]$ and the full flux range, respectively.

4 ADDING THE FLUX POWER SPECTRUM

In this section, we first revisit constraints from the SDSS flux PS alone before proceeding to combine this data set with the flux PDF of the UVES/VLT data for a joint analysis. The SDSS flux PS is based on 3035 QSO spectra with low resolution and low S/N, spanning the redshift range $z = 2.2$–4.2 (measurements are made at 11 wavenumbers in 12 redshift bins). Dealing with the systematic uncertainties of low-resolution and low-S/N QSO spectra and extracting the flux power are a difficult task. We refer to McDonald et al. (2005) for a comprehensive study of the removal of continuum fluctuations, metal line contamination, damped Lyman α systems and dealing with the resolution of the spectrograph and noise level in each of the redshift bins. All these effects need to be properly taken into account, as a poor treatment would impact the obtained flux power in a non-trivial way. In the following, we will use the flux power provided by the SDSS collaboration, introducing 'nuisance parameters' for the resolution and noise in each redshift bin as suggested by McDonald et al. (2005), and implicitly assuming that all the contaminants above have been either removed or properly modelled.

We compute the constraints from the SDSS flux PS in a similar way to Viel & Haehnelt (2006) with the notable difference that we calculate the predicted flux statistics by expanding around a model with $\gamma \sim 1$ in the redshift range $z = [2$–$4]$, while the original analysis was based on simulations with $\gamma \sim 1.6$. Furthermore, the flux power is computed using a Taylor expansion to second instead of first order. The parameters of the fiducial cosmological simulation are those of the B2 model in Viel & Haehnelt (2006). As before the flux statistics have been corrected for box-size and resolution effects. We compute the derivatives required for the Taylor expansion by performing between four and six hydrodynamical simulations for every cosmological and astrophysical parameter considered. In addition, we now allow for the effect of the reionization redshift, $z_{\rm re}$, and introduce this as an extra parameter. We interpolate between two very different reionization histories with $z_{\rm re} \sim 15$ and 7. We also introduce two extra parameters describing the redshift evolution of the thermal state of the IGM, the power-law index of the T and γ relations at $z > 3$ (a redshift range which is not probed by the PDF).

The results for the PS-only analysis are summarized in the first two columns of Table 2 for a low-redshift-only sample, $z = [2.2$–$3.6]$, and the full SDSS data set, $z = [2.2$–$4.2]$. We decided to perform a separate analysis which omits the highest redshift bins following Viel & Haehnelt (2006), who obtained a somewhat poorer fit for the high-redshift ($z > 3.6$) PS estimates. Despite the fact that the flux statistics were calculated by expanding around a reference model with very different thermal history, in both instances the analysis still gives constraints on the cosmological parameters that are in agreement with the previous analysis of Viel & Haehnelt (2006). This is rather reassuring. However, there are some aspects of the results that need scrutiny. First, we note that for the flux power only the temperature at mean density, T_0, is significantly higher than that preferred by the PDF (and higher than expected for the photoionized IGM). Secondly, the value of σ_8 is now somewhat on the lower end of values allowed by the previous analysis of Lyman α data and thus in better agreement with the CMB data (e.g. Komatsu et al. 2009). This is due to the degeneracy between σ_8 and γ discussed in B08; allowing for $\gamma < 1$ means that the flux power can now be fitted by a slightly lower σ_8 (but, note that other parameters also have a significant influence on the inferred σ_8, most notably the mean flux level).

Table 2. Cosmological and astrophysical parameters derived from the $B2_1$ model ($\gamma \sim 1$) for the flux PS: (low z) flux PS fitted in the range $z = [2.2$–$3.6]$; (all z) flux PS fitted in the range $z = [2.2$–$4.2]$. The probability of having a χ^2 value larger than this for model $B2_1^{(\rm low\,z)}$ is 64 per cent, while for model $B2_1^{(\rm all\,z)}$ it is 12 per cent. The constraints for a joint analysis of flux PS and PDF ($F = 0.1$–0.8) are shown in the third column (probability is 35 per cent).

Parameter	$B2_1^{(\rm low\,z)}$	$B2_1^{(\rm all\,z)}$	$B2_1^{(\rm low\,z)} + (20{,}256)^{0.1-0.8}$
σ_8	0.85 ± 0.05	0.86 ± 0.04	0.90 ± 0.02
$n_{\rm s}$	0.93 ± 0.03	0.96 ± 0.02	0.95 ± 0.02
$\Omega_{0\rm m}$	0.25 ± 0.04	0.26 ± 0.03	0.25 ± 0.03
H_0	78 ± 7	77 ± 7	80 ± 5
T_0	38 ± 7	42 ± 6	26 ± 4
T_0^{s1}	-0.6 ± 1.3	-0.3 ± 1.1	1.4 ± 0.5
T_0^{s2}	-2.3 ± 1.3	-3.9 ± 1.3	-3.1 ± 1.5
γ^A	0.63 ± 0.50	0.79 ± 0.51	$0.50 \pm 0.\ 20$
γ^{s1}	-0.7 ± 2.6	0.4 ± 2	-2.1 ± 1.6
γ^{s2}	-1.2 ± 2.1	-1.4 ± 1.5	-1.4 ± 1.6
$\tau_{\rm eff}^A$	0.326 ± 0.028	0.322 ± 0.028	0.320 ± 0.007
$\tau_{\rm eff}^{s1}$	3.19 ± 0.25	3.25 ± 0.23	3.12 ± 0.10
$z_{\rm re}$	11.9 ± 3.8	9.1 ± 2.7	14.3 ± 3.6
χ^2/d.o.f.	78.9/85	139.7/121	136/130

Overall, the results from the new flux PS analysis are consistent with those inferred from the PDF alone except for the value of T_0 at $z = 3$, which is several σ above that inferred from the best fit to the flux PDF. In the last column of Table 2, we show the constraints for a joint analysis of flux PDF and PS. Somewhat surprisingly, the joint analysis prefers a larger value of $\sigma_8 = 0.9 \pm 0.02$ with rather small errors. We explicitly checked that this large value of σ_8 is related to the rather different T_0^A values that the PDF and PS favour. If we artificially remove the constraint of the temperature being simultaneously consistent with the somewhat discrepant temperatures favoured by the flux PDF and PS, the joint analysis gives $\sigma_8 = 0.86 \pm 0.03$ with an improvement of $\Delta\chi^2 = 12$. A not yet accounted for systematic error in the measurement of the flux PDF and/or PS appears to be a possible explanation for this discrepancy. Alternatively, the inconsistencies may suggest that a power-law $T-\rho$ relation is a poor approximation to the thermal state of the IGM and a wider range of physically motivated relations should be considered in future simulations.

5 DISCUSSION

We have presented cosmological and astrophysical constraints derived from the K07 Lyman α flux PDF measured from a set of 18 high-resolution QSO spectra whose statistical and systematic errors have been carefully estimated. The Lyman α flux PDF on its own provides tight constraints on the thermal state of the IGM and on cosmological parameters describing the linear dark matter PS. The results have been obtained by fitting the flux PDF at three different redshift bins in the range $2 < z < 3$ and for three different flux ranges $F = [0.1$–$0.8]$, $[0$–$0.9]$ and $[0$–$1]$. There is a good agreement between the analyses for the full flux range and the two restricted flux ranges and the results are consistent with those derived in the simpler analysis made by B08. An inverted temperature–density relation is favoured at the $\sim 3\sigma$ level (at $z \sim 3$) if we consider the PDF for the full flux range, but the significance is reduced to 1–1.5σ if we restrict the analysis to $F = [0.1$–$0.8]$. The constraints for other

parameters are in agreement with those presented in the literature (e.g. the SDSS flux power in McDonald et al. 2005). We have also refined the method used by Viel & Haehnelt (2006) and updated the constraints from the SDSS flux PS. The constraints from the flux PS are consistent with those from the flux PDF, with the exception that the flux PS prefers a significantly larger temperature at mean density, T_0. A joint PS–PDF analysis gives a reasonable fit to the data but results in a larger σ_8 than an analysis of CMB data alone. This discrepancy appears to be related to the higher T_0 that the flux PS prefers.

Recent simulations of photoheating during He II reionization indicate that an inverted $T-\rho$ relation is very difficult to achieve within the standard model describing the thermal state of the IGM even if radiative transfer effects are taken into account, at least if He II reionization is driven primarily by QSOs (McQuinn et al. 2009; Bolton, Oh & Furlanetto 2009a). It therefore appears difficult to reproduce the observed flux PDF without invoking a not-yet-identified source of IGM heating, or additional systematic errors which impact on the flux PDF. Similarly, the high T_0 values preferred by the PS are very difficult to reconcile with constraints from the widths of thermally broadened absorption lines (e.g. Ricotti et al. 2000; Schaye et al. 2000) and our understanding of the heating of the photoionized IGM.

As the results from the flux PDF and the CMB data agree very well, the rather high values of T_0 preferred by the flux PS suggest perhaps instead that we have identified a not yet accounted for systematic error in the SDSS flux PS data. Independent analysis based on line statistics, on new data sets at medium and high resolution and further progress in incorporating He II reionization models into high-resolution hydrodynamical simulations will hopefully allow us to further improve our understanding of the systematic uncertainties of Lyman α forest data and resolve these small but statistically significant inconsistencies.

ACKNOWLEDGMENTS

Numerical computations were performed on the COSMOS supercomputer at DAMTP and on the High Performance Computer Cluster Darwin in Cambridge (UK). COSMOS is a UK-CCC facility which is supported by HEFCE, PPARC and Silicon Graphics/Cray Research. Part of the analysis was also performed at CINECA (Italy) with CPU time assigned thanks to an INAF-CINECA grant. We thank A. Lidz and P. McDonald for suggestions and useful criticism.

REFERENCES

Becker G. D., Rauch M., Sargent W. L. W., 2007, ApJ, 662, 72
Bolton J. S., Becker G. D., 2009, MNRAS, in press (arXiv:0906.2861)
Bolton J. S., Haehnelt M. G., Viel M., Springel V., 2005, MNRAS, 357, 1178
Bolton J. S., Oh S. P., Furlanetto S. R., 2009a, MNRAS, 395, 736
Bolton J. S., Oh S. P., Furlanetto S. R., 2009b, 396, 2405
Bolton J. S. et al., 2008, MNRAS, 386, 1131 (B08)
Croft R. A. C. et al., 2002, ApJ, 581, 20
Desjacques V., Nusser A., Sheth R. K., 2007, MNRAS, 374, 206
Jena T. et al., 2005, MNRAS, 361, 70
Kim T. et al., 2007, MNRAS, 382, 1657 (K07)
Komatsu E. et al., 2009, ApJS, 180, 330
Lesgourgues J., Viel M., Haehnelt M. G., Massey R., 2007, J. Cosmol. Astropart. Phys., 11, 8
Lidz A. et al., 2006, ApJ, 638, 27
McDonald P. et al., 2000, ApJ, 543, 1
McDonald P. et al., 2005, ApJ, 635, 761
McQuinn M. et al., 2009, ApJ, 694, 842
Meiksin A., Bryan G., Machacek M., 2001, MNRAS, 327, 296
Meiksin A. A., 2007, preprint (arXiv e-prints)
Pawlik A. H., Schaye J., van Scherpenzeel E., 2009, MNRAS, 394, 1812
Rauch M., 1998, ARA&A, 36, 267
Rauch M. et al., 1997, ApJ, 489, 7
Ricotti M., Gnedin N. Y., Shull J. M., 2000, ApJ, 534, 41
Schaye J. et al., 2000, MNRAS, 318, 817
Seljak U., Slosar A., McDonald P., 2006, J. Cosmol. Astropart. Phys., 10, 14
Springel V., 2005, MNRAS, 364, 1105
Theuns T. et al., 1998, MNRAS, 301, 478
Tytler D. et al., 2004, ApJ, 617, 1
Viel M., Haehnelt M. G., 2006, MNRAS, 365, 231
Viel M., Haehnelt M. G., Springel V., 2004, MNRAS, 354, 684
Viel M. et al., 2008, Phys. Rev. Lett., 100, 041304
Viel M. et al., 2009, MNRAS, 393, 774
Zaroubi S. et al., 2006, MNRAS, 369, 734

This paper has been typeset from a TEX/LATEX file prepared by the author.